Enhanced Water Vapor Absorption Within Tropospheric Clouds: A Partial Explanation for Anomalous Absorption

David Crisp and Cinzia Zuffada
Jet Propulsion Laboratory California Institute of Technology, Pasadena, CA 91109
dc@crispy.jpl.nasa.gov

ABSTRACT

Comparisons between solar flux measurements and predictions obtained from theoretical radiative transfer models indicate that most of these models underestimate the globally-averaged solar energy absorbed by cloudy atmospheres by up to 25 W m^{-2}. The origin of this anomalous absorption has not yet been established, but it has been attributed to a variety of sources including oversimplified or missing physical processes in the existing models, uncertainties in the input data, and even measurement errors. Here, we used a sophisticated atmospheric radiative transfer model to provide improved constraints on the physical processes that contribute to the absorption of solar radiation by the Earth's atmosphere. We find that the amount of sunlight absorbed by a cloudy atmosphere is inversely proportional to the solar zenith angle and the cloud top height, and directly proportional to the cloud optical depth and the water vapor concentration within the clouds. Atmospheres with saturated, optically-thick, low clouds absorbed about 12 W m^{-2} more than clear atmospheres. This accounts for about 1/2 to 1/3 of the anomalous absorption. Atmospheres with optically thick middle and high clouds usually absorb less than clear atmospheres. Because water vapor is concentrated within and below the cloud tops, this absorber is most effective at small solar zenith angles. An additional absorber that is distributed at or above the cloud tops is needed to produce the amplitude and zenith angle dependence of the observed anomalous absorption.

1. INTRODUCTION

Averaged over the globe and over the annual cycle, the Earth receives about 342 W m^{-2} from the sun. About 30% of this solar energy ($\sim$102 W m^{-2}) is scattered back to space by the surface and atmosphere, while the remaining 240 W m^{-2} is absorbed by this system. The partitioning of this energy between the surface and atmosphere is not completely understood, however. In particular, recent compilations of the solar flux measurements collected at the surface and at the top of the atmosphere (cf. Li et al., 1996 and references therein) indicate that the atmosphere absorbs as much as 98 W m^{-2}, while the radiative transfer algorithms used in global general circulation models (GCMs) indicate values between 56 and 68 W m^{-2} (Arking, 1996). Aircraft observations collected simultaneously at different altitudes also show that the atmosphere absorbs significantly more solar radiation than existing models predict (Piewskie and Valero, 1995). The largest discrepancies are seen in cloudy regions, where the atmosphere appears to absorb up to 50% more sunlight than otherwise comparable cloud-free regions. In contrast, most models indicate similar amounts of absorption in cloudy and clear-sky regions. Because the largest discrepancies are seen in cloudy conditions, this phenomena has come to be known as the *cloud absorption anomaly* (Wiscombe, 1995; Li et al., 1996; Cess et al., 1995; Ramanathan et al., 1995). The amplitude of this anomalous absorption is usually expressed in terms the net shortwave cloud forcing,

$$R = \frac{C_{ss}}{C_{st}} = \frac{F_s^{all} - F_s^{clr}}{F_t^{all} - F_t^{clr}}$$

where C_{ss} and C_{st} are the shortwave cloud forcings at the surface (s) and at the top of the atmosphere (t). These quantities are obtained by subtracting the net fluxes for co-located cloudy (all) and clear (clr) soundings. With this definition, R describes changes in solar absorption by the entire cloudy column, and not just the cloud alone.

The observations described by Cess et al. (1995), Ramanathan et al. (1995), and Piewskie and Valero (1995) indicate values of R near 1.5 at all locations where measurements were obtained, while the radiative transfer algorithms used in most GCMs find $R \sim 1.0$. Other observational studies also find values of R near 1.5 in the tropics, but show significant spatial and seasonal variations, with somewhat lower values at mid and high latitudes (Li et al. 1996). Other analysis efforts indicate that the anomalous absorption is actually more strongly correlated with the column water vapor abundance than cloud amount (Arking, 1996). In any case, these large uncertainties in the amplitude and vertical distribution of solar energy have raised concerns about our understanding of the solar forcing of the climate system.

Several plausible sources for this anomalous absorption have been proposed, but its origin has not yet been identified. The most detailed modeling studies to date have focused on the effects of enhanced absorption by cloud particles (Chou et al. 1995; Lubin et al., 1996), or by absorbing aerosols embedded within and below the clouds (c.f. Li et al. 1996). Chou et al. (1995) showed that globally-averaged cloud forcing ratios as large as 1.5 are obtained only when the cloud particle absorption is increased by factors as large as 40, but the constituents responsible for these large increases were not specifically identified. Lubin et al. (1996) found that near-infrared ($1.6\mu m$) absorption by large ice crystals ($r > 100\mu m$) could also produce values of R as large as 1.5 for small solar zenith angles, but this forcing decreased much more rapidly with solar zenith angle than the observed values. Others have proposed that cloud absorption anomaly may be related to horizontal inhomogeneities in the clouds, which are omitted in most existing radiative transfer models (Stevens and Tsay, 1990), but this hypothesis has not yet been confirmed.

Another plausible candidate for this absorption is water vapor. State-of-the art radiative transfer models employed in GCMs use simplified algorithms to compute the absorption by this gas at near-infrared wavelengths (0.7 to 3.2 μm), because explicit, spectrum-resolving (line-by-line) methods are far too time consuming for global calculations at wavelengths where both multiple scattering and line absorption contribute to the extinction of sunlight. Many of these algorithms have been validated against more rigorous line-by-line models for clear-sky conditions, but their accuracy in cloudy conditions is largely unknown. Another factor that may contribute to underestimates of the water vapor absorption within clouds is the omission of continuum absorption between major bands. This absorption is often neglected at near-infrared wavelengths because it is relatively weak. However continuum absorption might play a significant role within low clouds, where the water vapor concentrations are large, and multiple scattering can significantly enhance the absorber pathlength. Finally, most detailed studies of anomalous absorption have used background water vapor mixing ratios (McClatchey 1972) in both cloudy and cloud-free atmospheres (Li et al., 1996; Chou et al., 1995). Real clouds are usually saturated with water vapor. This simplification alone will result in an underestimate of water vapor's contribution to the cloud absorption anomaly.

Here, we used a sophisticated, spectrum-resolving, atmospheric radiative transfer model to provide a more comprehensive assessment of the role of near-infrared water vapor absorption in cloudy atmospheres. This model explicitly accounts for all radiative processes that are known to contribute to the extinction of solar radiation in vertically-inhomogeneous, plane-parallel, scattering, absorbing atmospheres. It was used to compute the wavelength-dependent solar intensities as a function of altitude for a variety of clear and cloudy model atmospheres. These results were integrated over wavelength and angle to yield bolometric solar fluxes and heating rates.

2. METHODS

The modeling methods used here include a line-by-line model for gas absorption, single scattering algorithms for cloud droplets and ice crystals, and a spectrum-resolving atmospheric radiance model that incorporates a multi-level, multi-stream, discrete ordinate algorithm (Stamnes et al. 1988) and high resolution spectral mapping methods (Meadows and Crisp, 1996). These methods were used to generate level-dependent synthetic spectra at wavelengths between 0.125 and $8.3\mu m$ (1200 80000 cm^{-1}) for a variety of cloudy and clear model atmospheres. The line-by-line model was used to generate monochromatic gas absorption coefficients for H_2O, CO_2, O_3, N_2O, CH_4, CO, and O_2 at 62 levels between the surface and 80km. This model employs an efficient, multi-grid algorithm that completely resolves the cores of gas absorption lines at all atmospheric levels, and includes their contributions at large distances (1000 cm^{-1}) from the line centers (c.f. Meadows and Crisp, 1996). H_2O continuum absorption was included explicitly by using the far-wing line shape function recommended by Clough et al. (1989). To determine the effects of this continuum, a special set of H_2O absorption coefficients were generated with a 25 cm^{-1} line cut-off. Line parameters were obtained from the HITRAN 96 database (Rothman et al. 1992). The single-scattering optical properties of liquid water droplets were computed with a Mie scattering model (c.f. Meadows and Crisp, 1996). Cirrus clouds were parameterized as polydispersions of hexagonal crystals, and their optical properties were derived using geometric optics (Muinonen et al. 1989). The liquid water and ice refractive indices were obtained from Segelstein (1981) and Warren, (1984), respectively. The moderate-resolution solar spectrum compiled by C. Wehrli (WCRP Publication Series No. 7, WMO ITD-No. 149, pp 119-126, October 1986) was used for all simulations. Wavelength-dependent surface albedos for a moderately rough ocean surface ($0.05 \leq a \leq 0.07$) were used for all simulations.

The McClatchey (1972) mid-latitude summer (MLS) profile was used in all experiments presented here. The nominal MLS gas mixing ratios were used for all gases except for H_2O. The MLS water vapor mixing ratios were used only for the clear-sky and "Dry" cloud simulations. For the "saturated" cloudy cases, the water vapor mixing ratios were increased to

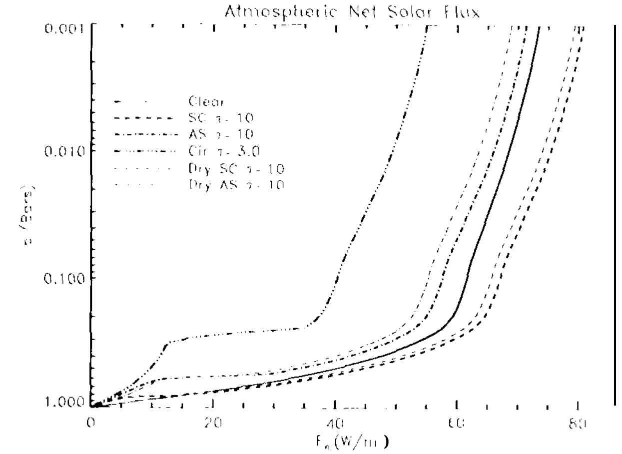

Figure 1: (a) Global average atmospheric net fluxes (defined by subtracting the net downward flux at the surface from the flux at each level) for a clear MLS atmosphere, and for atmospheres with a single Cirrus (Cir), Altostratus (AS), or Strato Cumulus (SC) cloud. The thick dashed and dash-dot lines are for saturated SC and AS clouds, while the thin dashed and dash-dot lines are for SC and AS clouds with MLS H_2O mixing ratios. If cloud liquid water absorption is neglected (ω_o= 1), the atmospheric absorption falls by ~4 W m^{-2} for SC (1011(1S and 7 W m^{-2} for AS (101](1S.

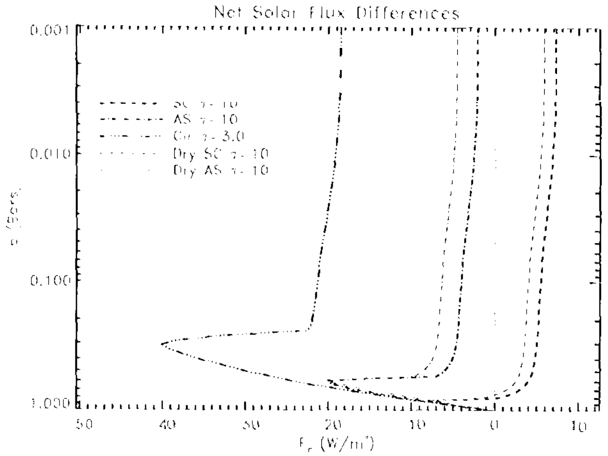

Figure 2: Differences between cloudy and clear-sky net fluxes for the atmospheres listed in Figure 1. In cloudy atmospheres, the absorption of reflected sunlight by the weak O_3 Huggins and Chappuis bands enhances the flux divergence at stratospheric levels.

their saturation values within the clouds. The cloudy model atmospheres included a single, plane-parallel cirrus (0.1 < τ_v < 10, 7 ≤ z < 10 km), altostratus (0.3 ≤ τ_v ≤ 60, 3.6 < z < 4.8 km), or stratocumulus (0.3 ≤ τ_v ≤ 60, 1.0 ≤ z ≤ 1.5 km) cloud layer. No aerosols were included in these calculations. Radiance spectra were derived at 4 solar zenith angles (0, 30, 60, 85°), and these results were integrated over zenith angle to yield estimates of the globally-averaged values. The model atmospheres were divided into 61 layers between the surface and 80 km, and radiances were generated for 4 to 16 zenith angles at each level.

3. RESULTS AND CONCLUSIONS

Globally-averaged, bolometric solar fluxes for MLS atmospheres with and without clouds are shown in Figure 1. The differences between the net fluxes in cloudy and clear-sky cases are shown in Figure 2. In this particular example, which illustrates the effects of moderately thick clouds, the largest positive shortwave cloud radiative forcings are produced by an atmosphere with a single, horizontally-uniform, saturated, stratocumulus (SC) ('1011(1 deck. This atmosphere absorbs ~15 W m^{-2} more sunlight than the clear-sky case at levels above the cloud base, but it absorbs about 7.5 W m^{-2} less than the clear atmosphere at altitudes below the cloud base, to yield a net atmospheric cloud forcing of about 7.5 W m^{-2}. Water vapor (and to a lesser extent, liquid water) absorption within the cloud accounts for most of the additional flux divergence in cloudy atmospheres. At levels within the clouds, model atmospheres with saturated clouds include about 20% more water vapor than the "Dry" cloud cases, and absorb about 1.5 W m^{-2} more radiation. Water vapor continuum absorption contributes only about 1 W m^{-2} in both the clear and cloudy cases. Figure 3 shows that thin, saturated altostratus (AS) and stratocumulus (SC) clouds produce larger cloud forcing ratios than thicker clouds (like those described in Figures 1 and 2). However, this is largely an artifact of the definition of R, since C_{st} vanishes for thin clouds. Figure 4 shows that thicker clouds actually absorb more sunlight.

In general, we find that the amount of sunlight absorbed by cloudy atmospheres is inversely proportional to the solar zenith angle and the cloud top height, and directly proportional to the cloud optical depth and the water vapor mixing ratio within the cloud. The globally-averaged absorption in atmospheres with saturated, optically-thick, low clouds can exceed the clear sky absorption by 10 to 12 W m^{-2} (Figure 4). Atmospheres with optically thick middle and high clouds usually absorb less than clear atmospheres, but water vapor within and below optically-thin (τ < 1), saturated, altostratus layers can contribute 1 to 3% more absorption (~2 W m^{-2}) than that])10(111((,(1 by clear skies. Because the water vapor concentrations are usually greatest within and below the cloud tops, where scattering reduces the intensity of the solar flux, this constituent always])]()(111('(,(] its strongest absorption for small solar zenith angles. An additional absorber that is concentrated at or above the cloud tops is needed to produce a cloud shortwave forcing that is more independent of solar zenith angle, like that observed. The weakly-absorbing, uniformly-mixed, background tropospheric aerosols, which were

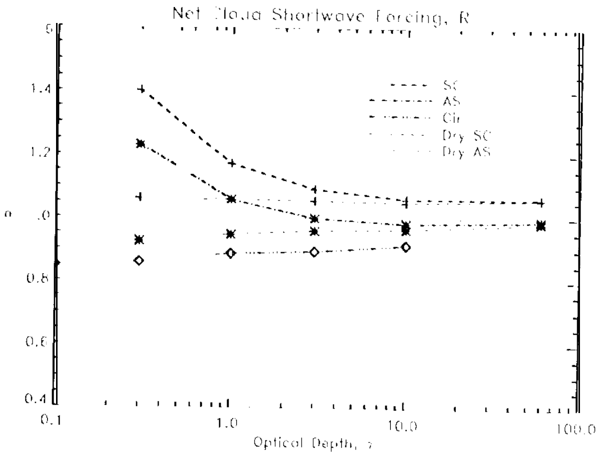

Figure 3: The global-average cloud shortwave forcing, R, is shown as a function of cloud optical depth, τ for the model atmospheres described in Figure 1. The largest values of R and the greatest sensitivity to water vapor absorption are seen for optically-thin clouds. This might explain why the largest values of R are often seen in regions with patchy clouds. Scattering of solar radiation by thin clouds does not significantly increase the planetary albedo, but can increase the pathlength for absorption at lower levels of the atmosphere.

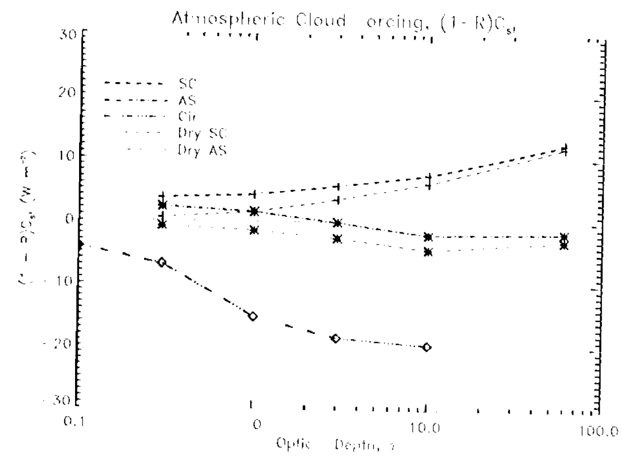

Figure 4: The global-average atmospheric absorption, $(1 - R)C_{st}$), is shown as a function of cloud optical depth, τ for the model atmospheres described in Figure 1. Even though the largest cloud shortwave forcings are obtained for small cloud optical depths, atmospheres with thicker clouds absorb more solar flux. The cloud forcing by thin clouds is much more sensitive to the water vapor abundance within and below the cloud.

omitted from these simulations, might provide this opacity.

4. REFERENCES CITED

Arking, A., 1996: Absorption of solar energy in the atmosphere: Discrepancy between model and observations, *Science, 273*, 779-782.

Cess, R. D. *et al.*, 1995: Absorption of solar radiation by clouds: Observations versus models, *Science, 267*, 496-499.

Chou, M. D., et al. 1995: The effect of clouds on atmospheric absorption of solar radiation, *Geophys. Res. Lett., 22*, 1885-188.

Clough, S. A., et al., 1989: Line shape and the water vapor continuum, *Atm. Res., 23*, 229-241.

Li, Z. and L. Moreau, 1996: Alteration of atmospheric solar radiation by clouds: Simulation and observation, *J. Appl. Met., 35*, 653-670.

Lubin, D., J.-P. Chen, P. Piewskie, V. Ramanathan, and P. J. Valero, 1996: Microphysical examination of excess cloud absorption in the tropical atmosphere, *J. Geophys. Res., 101*, 16961-16972.

McClatchey, R. et al., 1972: Optical properties of the atmosphere, *Environ. Res. Paper 411*, 110 pp.

Meadows, V. S. and D. Crisp, 1996: Ground-Based Near-Infrared Observations of the Venus Night-Side, *J. Geophys. Res., 101*, 4595-4622.

Muinonen, K., et al., 1989: Light Scattering by randomly-oriented crystals, *Appl. Opt., 28*, 3044-3050.

Piewskie, P. and F. P. J. Valero, 1995: Direct observation of excess solar absorption by clouds, *Science, 267*, 1626-1629.

Ramanathan *et al.*, 1995: Warm pool heat budget and shortwave cloud forcing: A missing physics? *Science, 267*, 499-503.

Rothman, L. S., *et al.*, 1992: The HITRAN molecular database: Editions of 1991 and 1992, *J. Quant. Spectrosc. Radiat. Transfer, 48*, 469-507.

Segelstein, D., 1981: The complex refractive index of water", M.S. Thesis, University of Missouri-Kansas City.

Stamnes, K., et al., 1988: Numerically stable algorithm for discrete-ordinate-method radiative transfer in multiple scattering and emitting layered media, *Appl. Opt., 27*, 2502-2509.

Warren, S., 1984: Optical constants of ice from the ultraviolet to the microwave, *Appl. Opt., 23*, 1206-1225.

Wiscombe, W. J., 1995: Atmospheric physics: An ab sorbing mystery, *Nature, 376*, 466-467.